Low-voltage PV power integration for variable frequency drives application

Shetty, Akshatha; Fernandes, B.G.; Ojo, Olorunfemi; Ferreira, J.A.

DOI
10.23919/EPE17ECCEEurope.2017.8099088

Publication date
2017

Document Version
Final published version

Published in
2017 19th European Conference on Power Electronics and Applications, EPE 2017 ECCE Europe

Low-voltage PV power integration for variable frequency drives application

Akshatha Shetty[1], B. G. Fernandes [1], Olorunfemi Ojo[2] and J A Ferreira[3]
[1] Department of Electrical Engineering
INDIAN INSTITUTE OF TECHNOLOGY BOMBAY
Powai, Mumbai 400076, India
Email: akshatha@iitb.ac.in, bgf@ee.iitb.ac.in
[2]Department of Electrical and Computer Engineering
TENNESSEE TECHNOLOGICAL UNIVERSITY
Cookeville, TN 38505. U.S.A
Email: jojo@tntech.edu
[3]DELFT UNIVERSITY OF TECHNOLOGY
The Netherlands
Email:j.a.ferreira@tudelft.nl

Acknowledgments

The authors would like to thank Department of Science and Technology (DST), Government of India for supporting this project.

Keywords

≪PWM rectifiers≫, ≪High gain DC-DC converters≫, ≪Grid connected PV systems≫, ≪Variable frequency drives≫, ≪Four leg converters≫.

Abstract

Renewable sources like solar photovoltaic (PV) are preferred to be operated at low voltages. This necessitates high voltage boosting when they have to be connected to the high voltage DC bus. Conventional DC-DC converters (eg. boost and buck-boost) offer high voltage gain at the cost of reduced efficiency. This paper proposes a novel method to integrate low voltage PV power to the high voltage DC bus using a simple boost converter. The analysis of the proposed topology and control strategies are discussed. Simulation studies are carried out in MATLAB/SIMULINK and results for the same are presented.

Introduction

Numerous requirements related to converters decide the choice of industrial drives. The focus is on solutions that present enhancements in performance parameters and physical dimensions [1]. As electric motor drive systems are the major consumers of energy, reducing their energy consumption contributes to significant energy savings [1]. Increased use of renewable sources at the consumer end is one of the promising solutions for curbing the energy crisis. Among the available renewable energy sources, PV energy is by far the most widely used source due to its eco-friendly nature and cost effectiveness. The traditional approach for integrating this power involves dedicated converters, which are connected to a common bus. The functionalities of these converters are two-fold (i) extract electrical energy from the renewable energy sources (ii) feed power to the common bus. To feed power to the common bus, the renewable sources can be integrated either on AC side or DC side. Invariably both the methods demand high gain voltage boosting, as renewable sources like solar photovoltaic (PV) are preferred to be operated at low voltages. The conventional boost DC-DC converters are widely employed for stepping up DC voltages due to its simple structure and many other advantages [2]. However, in this converter the

ratio of output voltage to input voltage cannot be significantly high. Hence the low voltage PV integration to a high voltage DC bus calls for a special high gain DC-DC converters [3] [4]. These special high gain topologies significantly increase the cost, size and weight as compared to the simple boost converter. Unified converters / multi-functional converters introduced in [5–7] for hybrid electric vehicles, use single converter to achieve multi-functionalities The inverter legs dedicated for the motor controller are used as the boost converter to step up the low voltage battery connected through the motor neutral, and the motor leakage inductance is utilised as a boost inductor, instead of a separate boost-up reactor. Thus motor windings will be carrying unified AC-DC current. This multi-frequency power transfer approach can considerably reduce the cost, weight and volume of the system. However, in this converter the voltage gain cannot be high [5–7].

Every voltage source inverter based variable frequency drive (VFD) has an AC to DC rectifier unit, which includes a large DC bus capacitor at the front end. Generally the PV source is integrated at the DC side in these applications [8]. Applying unified AC-DC concept for PWM rectifier can overcome the requirement of special high gain boost converters. The multi-frequency power transfer is possible, if a system maintains an unified AC-DC voltage at the point of common coupling and allows unified AC - DC current through it. The paper discusses a novel method of integrating a 202.5 V (Voc)/8.25 kW (HIP-190BA3) PV source into the 1250V DC bus of a 440V/55 kW (ACS800-37) drive system. The system uses a unified AC-DC approach to integrate low voltage PV energy into a high voltage DC bus. With this method a simple boost converter is used to perform the MPPT operation and low voltage PV power is integrated using the same PWM rectifier, which is the part of the VFD. The work presented in this paper pertains to the development of multi-functional converter topology and its control for improved utilization of PV integrated to Variable Frequency Drives.

Three phase PWM rectifiers with unified AC-DC input

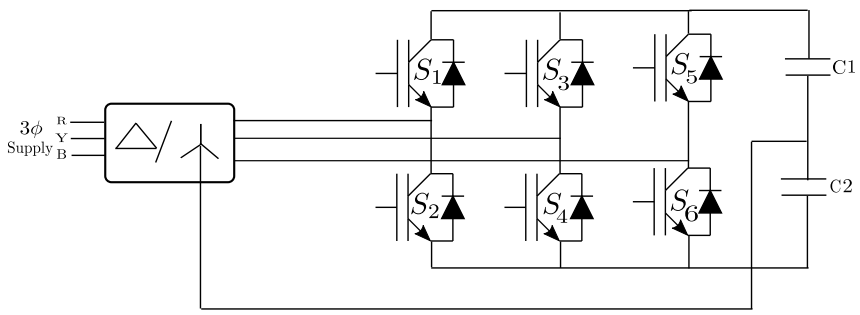

Fig. 1: Voltage source current controlled PWM rectifier

Generally, the input to a low voltage, high power drive system is fed from a three phase, 11kV/440V, 50 Hz transformer. One of the input stages of a three phase AC drive is shown in Fig. 1 [9]. In the proposed scheme (Fig. 2), the secondary of line transformer is modified to a zig-zag connection. The low voltage PV is connected through the neutral of the transformer, thus applying unified AC-DC voltage across the input of the AC to DC rectifier unit. The current through the PWM rectifier is controlled to draw both AC and DC currents, and the DC bus voltage is maintained at 1250 V. The zig-zag connection of the transformer avoids the core saturation due to DC currents. The transformer leakage inductance is used as the inductance between the source and the converter. This reduces a significant part of the overall size, weight and cost of the magnetic components in the unit.

As the input current is AC superimposed on DC, having the conventional three leg configuration (Fig. 1), this current shape will cause an unbalance in the output DC bus capacitor voltage. To avoid such an un-

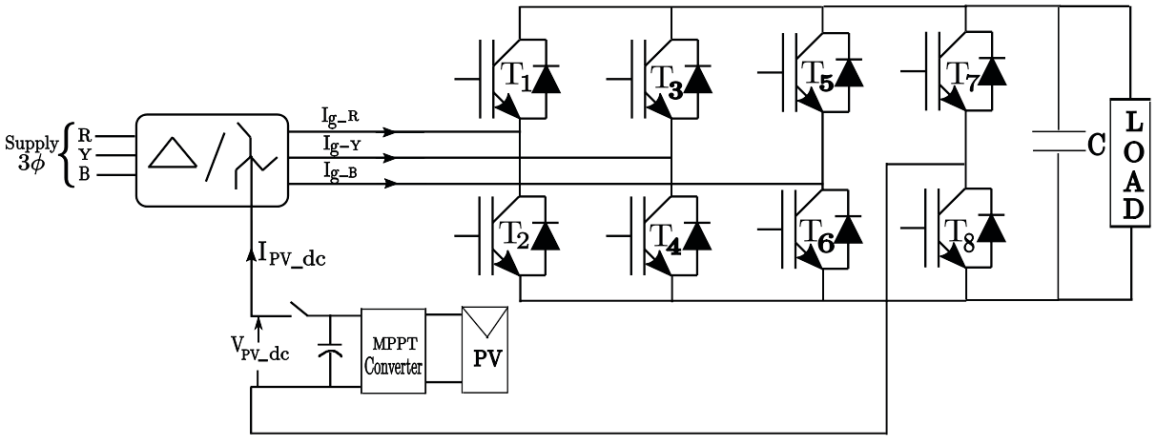

Fig. 2: Proposed PWM rectifier with PV integration

balance, a four leg configuration as shown in Fig. 2 is used. The four leg configuration can be decoupled into three single phase full bridge rectifier circuits [10]. The per phase circuit of the rectifier can be represented by the switching-cycle averaged model as shown in Fig. 3. The turn-on and turn-off sequences of a switching device are represented by an existence function. The existence function, S_{ij} =1 when it is turned on and S_{ij} =0, when it is off; where i represents the phase to which the device is connected and j signifies top (p) and bottom (n) device of the converter leg.

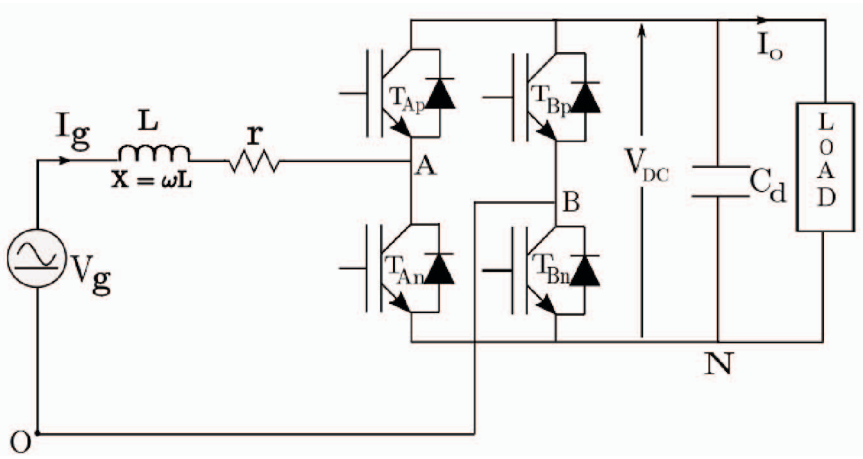

Fig. 3: Perphase model of three phase 4 leg PWM rectifiers

$$V_g = rI_g + LpI_g + V_{AB};$$

where $p = \frac{d}{dt}$

$$C_d pV_{DC} = I_g(S_{Ap} - S_{Bp})$$

$$V_{AO} = S_{Ap}(V_{DC} + V_{NO}) + S_{An}(V_{NO}) = S_{Ap}(V_{DC}) + V_{NO}$$

$$V_{BO} = S_{Bp}(V_{DC} + V_{NO}) + S_{Bn}(V_{NO}) = S_{Bp}(V_{DC}) + V_{NO}$$

$$V_{AB} = V_{AO} - V_{BO} = (S_{Ap} - S_{Bp})V_{DC}$$

$$V_g = V_{pv} + \Re\{V_{gg}e^{j\theta_e}\} \quad (1)$$

Where, V_{pv} = DC quantity and V_{gg} = complex phasor
Using harmonic balance technique,

$$I_g = I_{pv} + \Re\{I_{gg}e^{j\theta_e}\} \tag{2}$$

$$V_g = rI_g + LpI_g + V_{DC}(S_{Ap} - S_{Bp}) \tag{3}$$

Substituting (1) and (2) into (3) and comparing the components we get,

$$V_{pv} + \Re\{V_{gg}e^{j\theta_e}\} = r[I_{pv} + \Re\{I_{gg}e^{j\theta_e}\}] + Lp[I_{pv} + \Re\{I_{gg}e^{i\theta_e}\}] + [\Re\{Me^{j\theta_e}\}V_{DC} + V_p]$$

$$V_{AB} = (S_{Ap} - S_{Bp})V_{DC} = Mcos(\theta_e + \delta)V_{DC} + V_P$$

$$V_{pv} = rI_{pv} + LpI_{pv} + V_p$$

$$V_{gg} = rI_{gg} + j\omega LI_{gg} + LpI_{gg} + \hat{M}V_{DC}$$

At steady state condition,

$$I_{pv} = \frac{V_{pv} - V_p}{r}$$

$$V_{gg} = rI_{gg} + j\omega LI_{gg} + \hat{M}V_{DC}$$

Where, $\hat{M} = M\angle\delta^\circ$ and substituting, $V_{gg} = V_s\angle 0^\circ$ and $\hat{M}V_{DC} = V_2\angle\delta^\circ$

$$I_{gg} = \frac{V_s\angle 0^\circ - V_2\angle\delta^\circ}{j\omega L}$$

$S = V_{gg}I_{gg}^*$; from this we can write, $P_{ac} = \frac{V_sV_2sin\delta}{X}$ and $P_{dc} = V_{pv}I_{pv}$

Analysis of three phase PWM rectifier with unified AC-DC input

Fig. 4, shows the circuit topology of the four-leg voltage source AC/DC converter in which the fourth leg is connected through a PV source to the neutral of the three-phase transformer. Considering, V_{ao}, V_{bo}

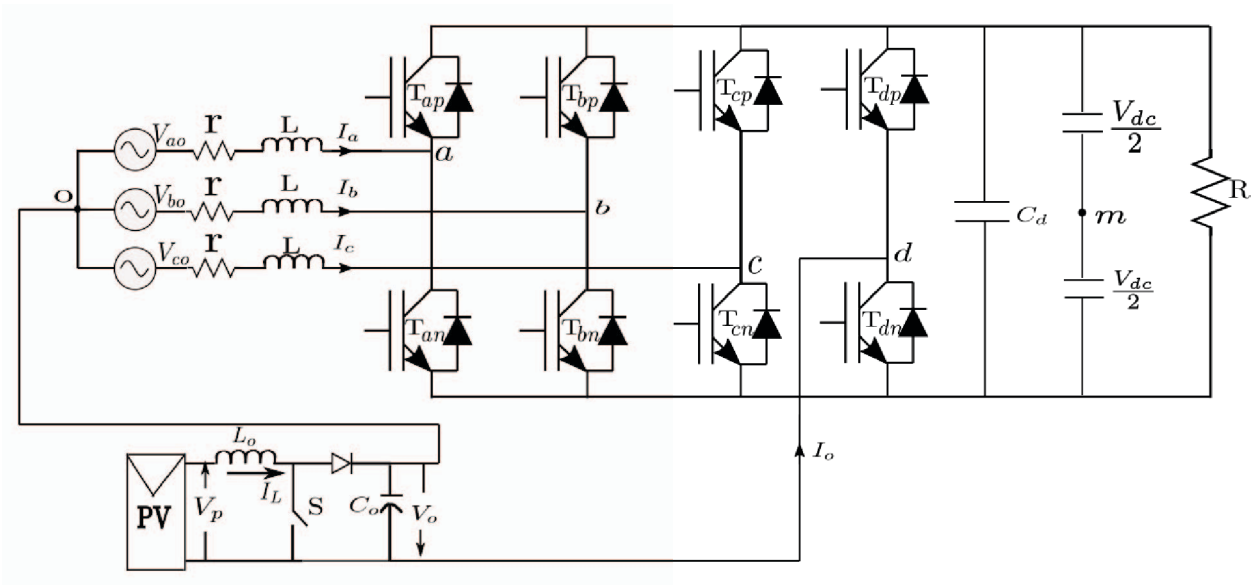

Fig. 4: Four leg PWM rectifier with PV integration

&V_{co} are balanced ; $I_a = I_{aa} - I_{oo}$, $I_b = I_{bb} - I_{oo}$, $I_c = I_{cc} - I_{oo}$; $I_a + I_b + I_c = -I_o$ and $I_{oo} = \frac{I_o}{3}$

From Fig. 4, the input voltage equations of the four-leg rectifier with PV integrated through the neutral is expressed in terms of the existence functions and output DC voltage V_{dc} and are given as

$$\begin{aligned} V_{ao} &= rI_a + LpI_a + \frac{V_{dc}}{2}S_{ap} - \frac{V_{dc}}{2}S_{an} + V_{mo} \\ V_{bo} &= rI_b + LpI_b + \frac{V_{dc}}{2}S_{bp} - \frac{V_{dc}}{2}S_{bn} + V_{mo} \\ V_{co} &= rI_c + LpI_c + \frac{V_{dc}}{2}S_{cp} - \frac{V_{dc}}{2}S_{cn} + V_{mo} \end{aligned} \tag{4}$$

$$\begin{aligned} V_{ao} &= rI_a + LpI_a + \frac{V_{dc}}{2}(2S_{ap} - 1) + V_{mo} \\ V_{bo} &= rI_b + LpI_b + \frac{V_{dc}}{2}(2S_{bp} - 1) + V_{mo} \\ V_{co} &= rI_c + LpI_c + \frac{V_{dc}}{2}(2S_{cp} - 1) + V_{mo} \end{aligned} \tag{5}$$

$$V_o = \frac{V_{dc}}{2}(2S_{dp} - 1) + V_{mo} \tag{6}$$

Subtracting, Eq (10) from Eq (9) we get,

$$\begin{aligned} V_{ao} - V_o &= rI_a + LpI_a + V_{dc}(S_{ap} - S_{dp}) \\ V_{bo} - V_o &= rI_b + LpI_b + V_{dc}(S_{bp} - S_{dp}) \\ V_{co} - V_o &= rI_c + LpI_c + V_{dc}(S_{cp} - S_{dp}) \end{aligned} \tag{7}$$

Where, $p = \frac{d}{dt}$

$$\begin{bmatrix} F_{qs} \\ F_{ds} \\ F_{os} \end{bmatrix} = K \begin{bmatrix} F_a \\ F_b \\ F_c \end{bmatrix} \qquad Where, K = \frac{2}{3}\begin{bmatrix} cos\theta & cos(\theta-\beta) & cos(\theta+\beta) \\ sin\theta & sin(\theta-\beta) & sin(\theta+\beta) \\ \frac{1}{2} & \frac{1}{2} & \frac{1}{2} \end{bmatrix}$$

$$\begin{bmatrix} F_a \\ F_b \\ F_c \end{bmatrix} = K^{-1} \begin{bmatrix} F_{qs} \\ F_{ds} \\ F_{os} \end{bmatrix} \qquad Where, K^{-1} = \begin{bmatrix} cos\theta & sin\theta & 1 \\ cos(\theta-\beta) & sin(\theta-\beta) & 1 \\ cos(\theta+\beta) & sin(\theta+\beta) & 1 \end{bmatrix}$$

Performing q-d transformations on (11) we get,

$$\begin{aligned} V_{qs} &= r_s I_{qs} + L_s p I_{qs} + \omega L_s I_{ds} + S_{qs} V_{dc} \\ V_{ds} &= r_s I_{ds} + L_s p I_{ds} - \omega L_s I_{qs} + S_{ds} V_{dc} \\ V_{os} &= -V_o = r_s I_{os} + V_{dc}\{\frac{1}{3}[S_{ap} + S_{bp} + S_{cp}] - S_{dp}\} \end{aligned} \tag{8}$$

Substituting, $S_{ip} = 0.5(1 + M_{ip})$, where i = a,b,c and $I_a + I_b + I_c = -I_o$

$$V_{os} = -V_o = r_s I_{os} + V_{dc}\{\frac{1}{3}[0.5(1+m_{ap}) + 0.5(1+m_{bp}) + 0.5(1+m_{cp})] - 0.5(1+M_{dp})\}$$

$$V_{os} = -V_o = r_s I_{os} + V_{dc}[\frac{-M_{dp}}{2}]$$

$$M_{dp} = \frac{2(V_o + r_s I_{os})}{V_{dc}} \tag{9}$$

Substituting $S_{qs} = \frac{m_{qs}}{2}$ and $S_{ds} = \frac{m_{ds}}{2}$ we get,

$$\begin{aligned}
V_{qs} &= r_s I_{qs} + + L_s p I_{qs} + \omega L_s I_{ds} + \frac{m_{qs}}{2} V_{dc} \\
V_{ds} &= r_s I_{ds} + L_s p I_{ds} - \omega L_s I_{qs} + \frac{m_{ds}}{2} V_{dc} \\
C_d p V_{dc} &= S_{ap} I_a + S_{bp} I_b + S_{cp} I_c + S_{dp}(I_o) - I_{Load} \\
C_d p V_{dc} &= 0.5[1 + m_{ap}] I_a + 0.5[1 + m_{bp}] I_b + 0.5[1 + m_{cp}] I_c + 0.5[1 + M_{dp}](I_o) - I_{Load} \\
C_d p V_{dc} &= 0.5 m_{ap} I_a + 0.5 m_{bp} I_b + 0.5 m_{cp} I_c + 0.5[I_a + I_b + I_c] + 0.5 M_{dp} I_o + 0.5 I_o - I_{Load} \\
0.5 m_{ap} I_a &= 0.5[cos(\theta) m_{qs} + sin(\theta) m_{ds} + m_{os}][cos(\theta) I_{qs} + sin(\theta) I_{ds} + I_{os}] \\
0.5[m_{ap} I_a + m_{bp} I_b + m_{cp} I_c] &= \frac{3}{4}[m_{qs} I_{qs} + m_{ds} I_{ds}] + \frac{3}{2}[m_{os} I_{os}]
\end{aligned} \tag{10}$$

Substituting m_{os}=0 and $I_a + I_b + I_c = -I_o$;

$$C_d p V_{dc} = \frac{3}{4}[m_{qs} I_{qs} + m_{ds} I_{ds}] + 0.5 M_{dp} I_o - I_{Load} \tag{11}$$

At steady state condition, considering unity power factor operation, I_{ds}=0, V_{ds}=0, V_{qs}=V_m and $I_o = 3I_{os}$,

$$V_p = (1 - S) V_o \tag{A}$$

$$I_L(1 - S) = 3 I_{os} \tag{B}$$

$$V_m = r_s I_{qs} + \frac{m_{qs}}{2} V_{dc} \tag{C}$$

$$0 = -\omega L_s I_{qs} + \frac{m_{ds}}{2} V_{dc} \tag{D}$$

$$-V_o = r_s I_{os} - \frac{V_{dc}}{2}(m_{dp}) \tag{E}$$

$$0 = \frac{3}{4}[m_{qs} I_{qs}] + 0.5 M_{dp} I_o - I_{Load} \tag{F}$$

From (D) we find

$$I_{qs} = \frac{m_{ds} V_{dc}}{2 \omega L_s} \tag{G}$$

Substituting I_{qs} in (F) we get,

$$m_{ds} = \frac{k 8 \omega L_s}{3 m_{qs} V_{dc}} \tag{H}$$

$$Where, k = [I_{load} - 0.5 M_{dp} I_o]$$

Substituting m_{ds} and I_{qs} in equation (C) we get,

$$\frac{V_{dc}}{2} m_{qs}^2 - V_m m_{qs} + \frac{4 r_s k}{3} = 0 \tag{I}$$

Solving for m_{qs} we get,

$$m_{qs} = \frac{V_m \pm \sqrt{V_m^2 - 4\{\frac{V_{dc}}{2}\}\frac{4r_s k}{3}}}{V_{dc}} \quad \text{(J)}$$

Substituting (J) in (H) we get m_{ds}

Table I: Simulation Parameters

S.No.	Parameters	Symbol	value	units
1	Per phase leakage inductance of the transformer	L	0.006	H
2	Per phase resistance of the transformer voltage	r	0.1	Ω
3	Output DC capacitor	C_d	1000	μF
4	Load resistance	R	28	Ω
5	Rated output power	P_{Load}	55	kW
6	Rated output DC link voltage	V_{DC}	1250	V
7	Input AC voltage (L-L)	V_{ac}	440	V
8	PV power	P_{PV}	8.25	kW
9	PV voltage connected in the neutral	V_o	200.0	V
10	Total PV current	I_o	41.25	A

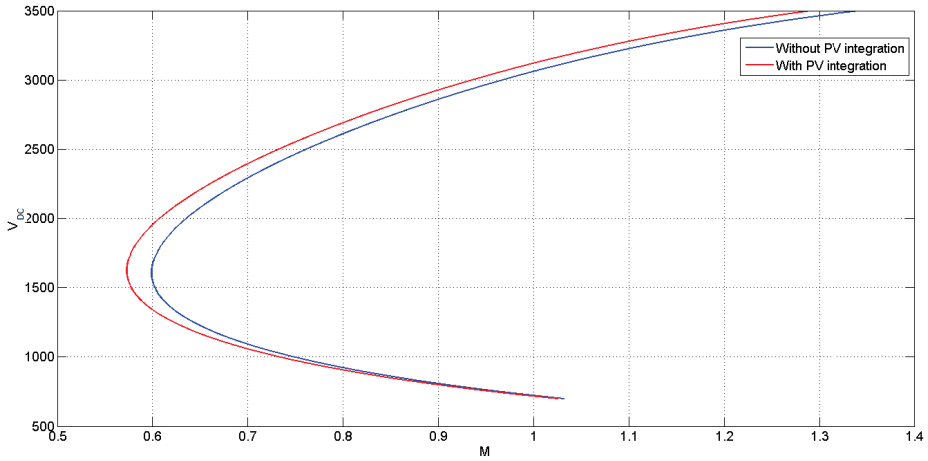

Fig. 5: Modulation Index vs DC bus voltage

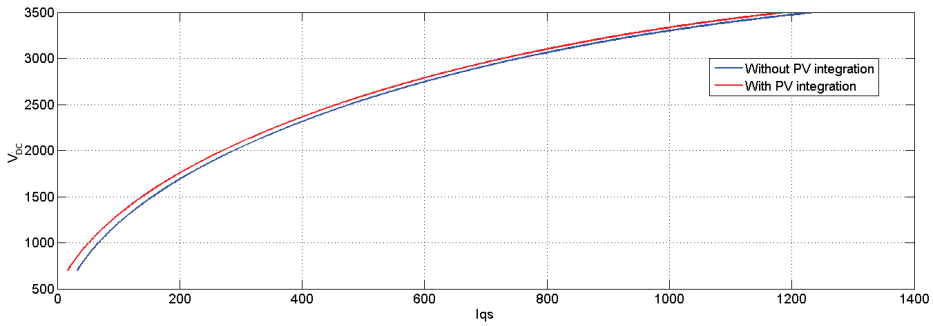

Fig. 6: Input peak AC current vs DC bus voltage

Control block diagram

The control block diagram is shown in Fig. 7. The active power requirement in the system is directly reflected as a change in the DC bus voltage V_{DC}. The output of the DC bus voltage (V_{DC}) controller is taken as the active current reference and Proportional Resonant (PR) controller is used for the inner current control. The input DC current reference, I_o is generated by maintaining the output voltage of the MPPT converter connected through the neutral of the zigzag transformer. The controller output used for maintaining the MPPT output voltage, V_o is used as the modulating waveform for the fourth leg. Depending upon the PV power availability, each phase input current will have both AC and DC components. Thus active power requirement of the load is shared by both grid and the PV.

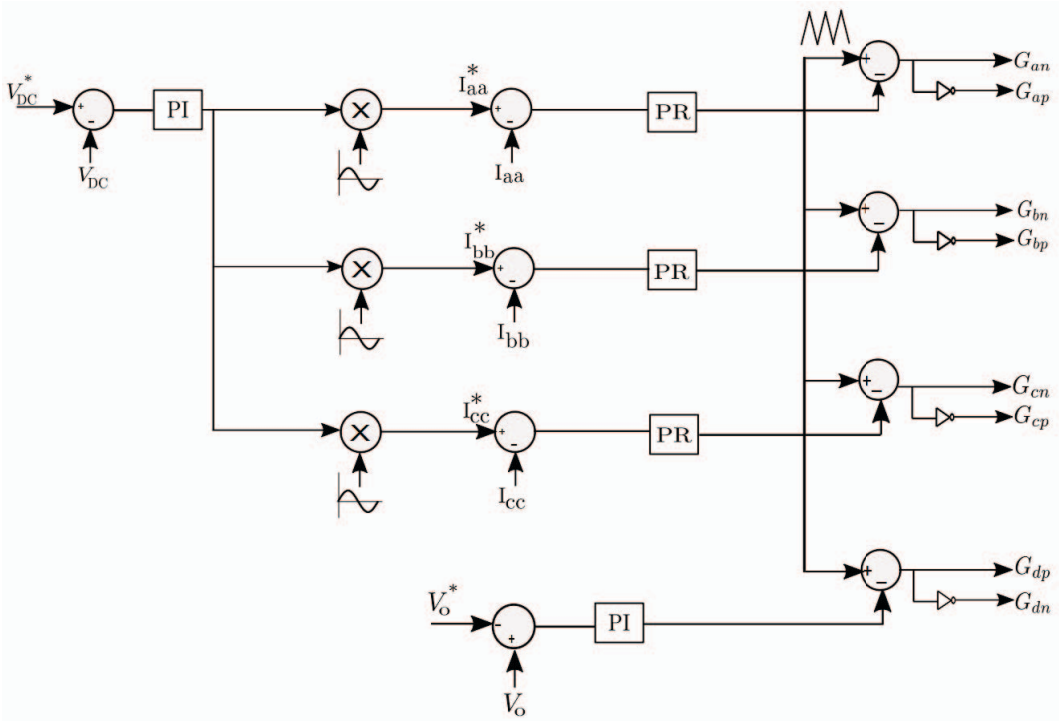

Fig. 7: Control block diagram for the PWM rectifier with unified AC -DC currents

Simulation Results

The proposed scheme for low voltage PV integration and control strategy is simulated on MATLAB / SIMULINK with simulation parameters shown in Table I. The output power from PV is fed to the converter through a zig-zag transformer. Fig. 8 shows the input three phase voltages, currents and output DC voltage of the proposed topology. Each phase current is composed of a 13.75 A of DC component and an RMS AC current of 60.98 A, transferring 55 kW of power to the load across the DC bus. Fig. 9 shows the harmonic spectrum of the input current through the 'R' phase. The spectrum shows that input current has 0Hz and 50Hz as the dominant frequency components. Fig. 10 shows the MPPT converter output voltage, current and the power. The output voltage of the MPPT converter is maintained at 200V delivering power of 8.25kW at 41.25A, using the fourth leg of the PWM rectifier.

Conclusion

PV integration leads to significant energy savings in large consumers of energy, such as electric motor drive systems. A novel topology of integrating PV power without requiring complex high gain boost converters is proposed. This offers the significant advantage of not requiring complex high gain boost converters. The performance of the proposed circuit topology and the control scheme is confirmed through simulation study using MATLAB/SIMULINK package.

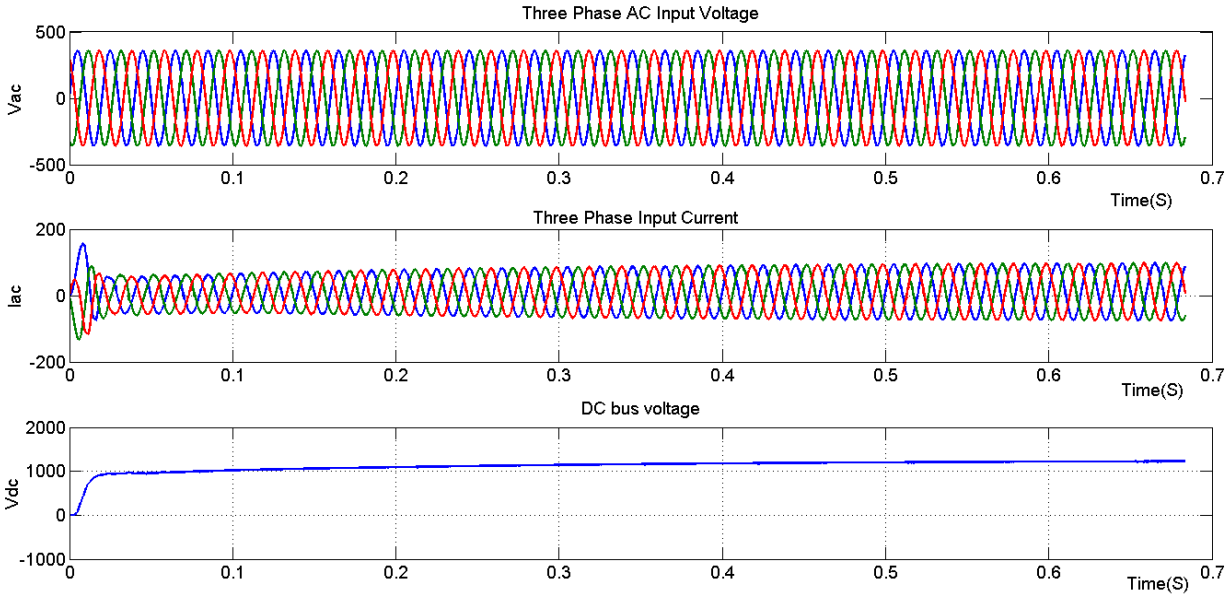

Fig. 8: Input voltage, input current and output DC voltage of the PWM rectifier with PV integration

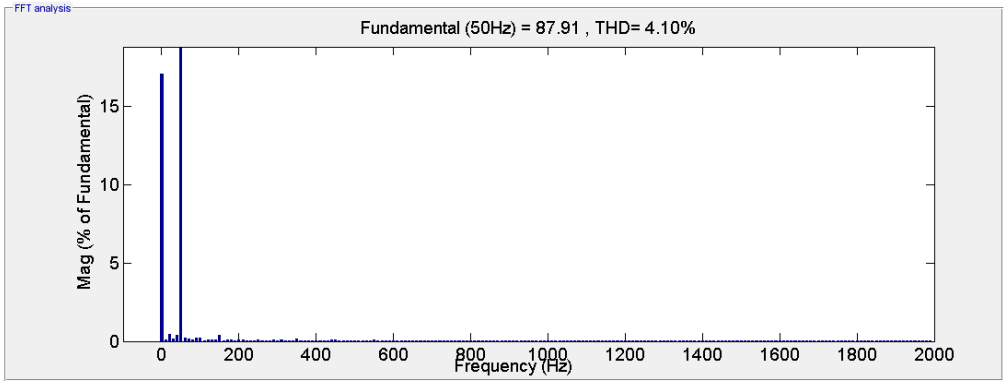

Fig. 9: Harmonic spectrum for the R phase current

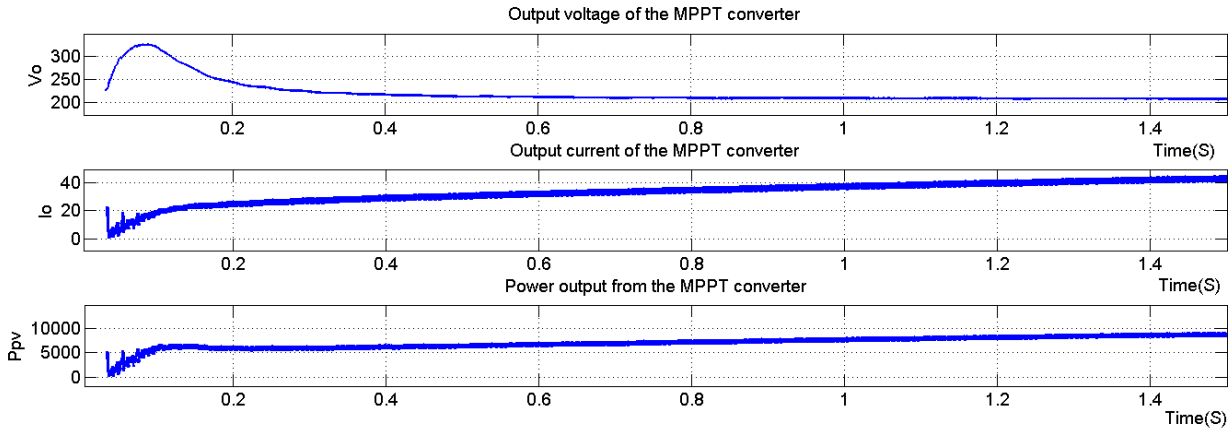

Fig. 10: Simulation results for PV voltage,current and power

References

[1] H. Abu-Rub, S. Bayhan, S. Moinoddin, M. Malinowski, and J. Guzinski, "Medium-voltage drives: Challenges and existing technology," *IEEE Power Electronics Magazine*, vol. 3, no. 2, pp. 29–41, June 2016.

[2] F. L. Tofoli, D. d. C. Pereira, W. J. de Paula, and D. d. S. Oliveira Jnior, "Survey on non-isolated high-voltage step-up dc-dc topologies based on the boost converter," *IET Power Electronics*, vol. 8, no. 10, pp. 2044–2057, 2015.

[3] M. Das and V. Agarwal, "Novel high-performance stand-alone solar pv system with high-gain high-efficiency dc-dc converter power stages," *IEEE Transactions on Industry Applications*, vol. 51, no. 6, pp. 4718–4728, Nov 2015.

[4] ——, "Design and analysis of a high-efficiency dc-dc converter with soft switching capability for renewable energy applications requiring high voltage gain," *IEEE Transactions on Industrial Electronics*, vol. 63, no. 5, pp. 2936–2944, May 2016.

[5] G. T. Chiang and J. i. Itoh, "Dc/dc boost converter functionality in a three-phase indirect matrix converter," *IEEE Transactions on Power Electronics*, vol. 26, no. 5, pp. 1599–1607, May 2011.

[6] J. I. Itoh and D. Ikarashi, "Investigation of a two-stage boost converter using the neutral point of a motor," *IEEE Transactions on Industry Applications*, vol. 49, no. 3, pp. 1392–1399, May 2013.

[7] K. Moriya, H. Nakai, Y. Inaguma, H. Ohtani, and S. Sasaki, "A novel multi-functional converter system equipped with input voltage regulation and current ripple suppression," in *Fourtieth IAS Annual Meeting. Conference Record of the 2005 Industry Applications Conference, 2005.*, vol. 3, Oct 2005, pp. 1636–1642 Vol. 3.

[8] S. Rajagopalan, A. Mansoor, J. Lai, and F. Khan, "Photovoltaic integrated variable frequency drive," US Patent App. 12/234,156, Mar. 15, 2010.

[9] J. R. Rodriguez, J. W. Dixon, J. R. Espinoza, J. Pontt, and P. Lezana, "Pwm regenerative rectifiers: state of the art," *IEEE Transactions on Industrial Electronics*, vol. 52, no. 1, pp. 5–22, Feb 2005.

[10] X. Chen, Z. Wei, H. Wang, C. Li, and C. Gong, "Research of three-phase four-leg rectifier," in *IECON 2012 - 38th Annual Conference on IEEE Industrial Electronics Society*, Canada,Oct 2012, pp. 719–724.